

New semi-analytical solutions for advection-dispersion equations in multilayer porous media

Elliot J Carr

Abstract A new semi-analytical solution to the advection-dispersion-reaction equation for modelling solute transport in layered porous media is derived using the Laplace transform. Our solution approach involves introducing unknown functions representing the dispersive flux at the interfaces between adjacent layers, allowing the multilayer problem to be solved separately on each layer in the Laplace domain before being numerically inverted back to the time domain. The derived solution is applicable to the most general form of linear advection-dispersion-reaction equation, a finite medium comprising an arbitrary number of layers, continuity of concentration and dispersive flux at the interfaces between adjacent layers and transient boundary conditions of arbitrary type at the inlet and outlet. The derived semi-analytical solution extends and addresses deficiencies of existing analytical solutions in a layered medium, which consider analogous processes such as diffusion or reaction-diffusion only and/or require the solution of complicated nonlinear transcendental equations to evaluate the solution expressions. Code implementing our semi-analytical solution is supplied and applied to a selection of test cases, with the reported results in excellent agreement with a standard numerical solution and other analytical results available in the literature.

Keywords advection dispersion reaction · analytical solution · layered media · Laplace transform

1 Introduction

Solute transport in porous media due to dispersion and groundwater flow is typically modelled using the advection-dispersion-reaction equation ([van Genuchten and Alves 1982](#); [Leij et al. 1991](#); [Liu et al. 1998](#); [Goltz and Huang 2017](#)). While solving this equation in heterogeneous porous media usually requires the application of numerical methods, analytical solutions are generally preferred when available as they are exact and continuous in space and time. The focus of this paper is analytical solutions for layered porous media, which are commonly observed in natural and constructed environments such as stratified soils and landfill clay liners ([Liu et al. 1998](#)). For this problem the transport coefficients (dispersion coefficient, retardation factor etc) are piecewise constant with the goal being to obtain the solute concentration in each layer as a function of space and time (see Figure 1).

Analytical solutions of advection-dispersion-reaction equations (and closely related equations such as advection-diffusion and reaction-diffusion equations) in layered media continue to attract interest ([Zimmerman et al. 2016](#); [Yang and Liu 2017](#); [Guerrero et al. 2013](#); [Carr and Pontrelli 2018](#); [Rodrigo and Worthy 2016](#)). Mainly due to their prevalence in heat conduction problems, most analytical solutions in the literature are developed for multilayer diffusion problems ([Carr and Turner 2016](#); [Carr and Pontrelli 2018](#); [Sun and Wichman 2004](#); [de Monte 2002](#); [Hickson et al. 2009](#); [Rodrigo and Worthy 2016](#)) with significantly less literature concerning advection-dispersion, reaction-diffusion or advection-dispersion-reaction problems.

Analytical solutions for advection-dispersion equations in layered media have been presented by a limited number of authors. Amongst the earliest work in this area is that of [Leij et al. \(1991\)](#), who applied the

Elliot J Carr

School of Mathematical Sciences, Queensland University of Technology (QUT), Brisbane, Australia.

E-mail: elliot.carr@qut.edu.au

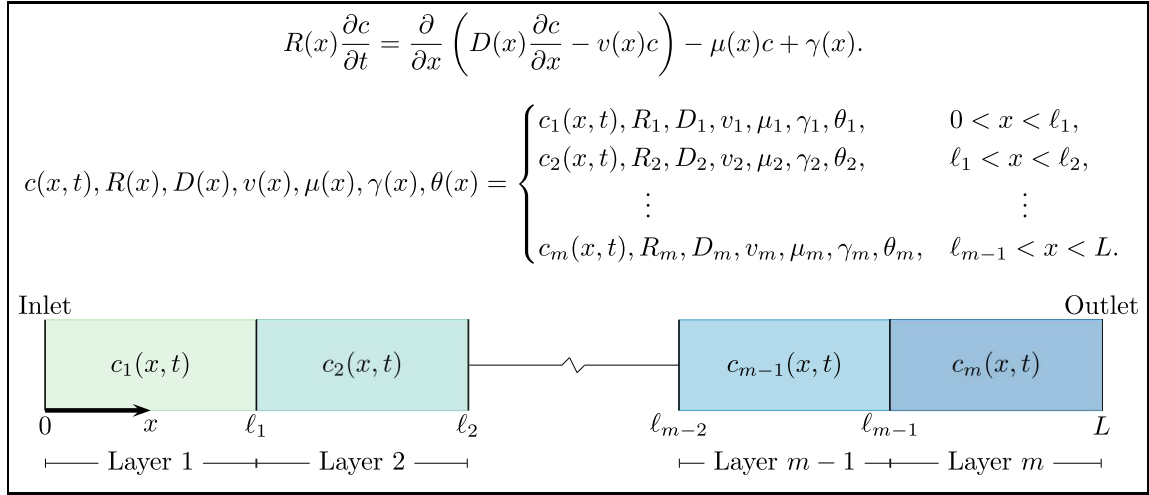


Fig. 1 Advection-dispersion-reaction in an m -layered medium. We solve for the concentration $c(x, t)$, where the retardation factor R , dispersion coefficient D , pore-water velocity v , volumetric water content θ and rate constants for first-order decay μ and zero-order production γ are constant within each layer but vary across layers. Continuity of concentration and dispersive flux are imposed at the interfaces between adjacent layers ($x = \ell_i$, $i = 1, \dots, m-1$) and transient boundary conditions of arbitrary-type are specified at the inlet ($x = 0$) and outlet ($x = L$).

Laplace transform to solve the advection-dispersion equation (with retardation factor) on a semi-infinite two-layer medium with finite first layer, semi-infinite second layer and continuity of concentration and dispersive flux at the interfaces between adjacent layers. Both concentration-type and flux-type boundary conditions were considered at the inlet and a zero concentration gradient was applied at the outlet (Figure 1). Exact expressions for the concentration in the Laplace domain were obtained and numerically inverted.

In follow up work, [Leij and van Genuchten \(1995\)](#) derived approximate analytical solutions by first expanding the Laplace domain concentration in both layers as infinite series, truncating each series after the first term and employing analytical inversion of the Laplace transform to convert the concentration back to the time domain. Subsequent analytical solutions for finite layered media and an arbitrary number of layers were derived by [Liu et al. \(1998\)](#) and then later by [Guerrero et al. \(2013\)](#), both using the method of eigenfunction expansion. [Liu et al. \(1998\)](#) considered the advection-dispersion equation and [Guerrero et al. \(2013\)](#) the advection-diffusion-reaction equation with a first order decay term. Both papers treated inlet boundary conditions of flux-type only with [Liu et al. \(1998\)](#) allowing for an arbitrary time-varying inlet concentration and [Guerrero et al. \(2013\)](#) a constant inlet concentration. Both approaches require a transcendental equation to be solved numerically for the eigenvalues with the accuracy of the solutions depending on the number of eigenvalues used in the expansions.

Recent work has revisited the use of Laplace transforms for solving multilayer transport problems due to the ease of treating different boundary conditions and the ability to avoid solving complicated nonlinear transcendental equations as required by eigenfunction expansion solutions ([Carr and Turner 2016](#)). Namely, [Carr and Turner \(2016\)](#) and [Rodrigo and Worthy \(2016\)](#) solved the multilayer diffusion problem using the Laplace transform for an arbitrary number of layers and various types of boundary and interface conditions. [Zimmerman et al. \(2016\)](#) solved a reaction-diffusion equation (without retardation factor) with a first order reaction term on a finite medium consisting of an arbitrary number of layers. All three of these papers ([Carr and Turner 2016](#); [Rodrigo and Worthy 2016](#); [Zimmerman et al. 2016](#)) introduce an unknown function of time at each interface, representing either the diffusive/dispersive flux or concentration, which allows the multilayer problem to be isolated and solved separately on each layer in the Laplace domain before being inverted back to the time domain.

Further relevant work involving the Laplace transform has focussed on the permeable reaction barrier-aquifer problem. In particular, semi-analytical solutions for the advection-dispersion-reaction equation have been developed by [Park and Zhan \(2009\)](#) for a semi-infinite one-dimensional medium using the Laplace transform and [Chen et al. \(2016\)](#) for a finite two-dimensional medium using Laplace and finite Fourier transforms. Both solutions are limited to two layers and numerically invert the Laplace transform using the [de Hoog et al. \(1982\)](#) algorithm.

The aim of the current paper is to extend, generalize and merge the work of Carr and Turner (2016), Rodrigo and Worthy (2016), Zimmerman et al. (2016) and Park and Zhan (2009) to solve advection-dispersion-reaction problems in one-dimensional media comprising an arbitrary number of layers using the Laplace transform. The derived solution is applicable to the most general form of linear advection-dispersion-reaction equation (van Genuchten and Alves 1982), a finite medium comprising an arbitrary number of layers, continuity of concentration and dispersive flux at the interfaces between adjacent layers and transient boundary conditions of arbitrary type at the inlet and outlet. To the best of our knowledge, analytical solutions satisfying all the above conditions have not previously appeared in the published literature. The derived solutions and resulting code supersedes our previous work on multilayer diffusion (Carr and Turner 2016; Carr and March 2018) by removing the requirement of numerically computing eigenvalues in each layer.

The remaining sections of this paper are organised as follows. In section 2 we describe the multilayer advection-dispersion-reaction problem considered in this work. Section 3 develops our proposed solution procedure using the Laplace transform. In section 4, the developed solutions are applied to a wide selection of test cases and compared to other analytical and numerical solutions available in the literature. In section 5, we summarise the work and discuss possible avenues for future research.

2 Multilayer transport model

We consider solute transport across an m -layered porous medium partitioned as $0 = \ell_0 < \ell_1 < \dots < \ell_{m-1} < \ell_m = L$ (Figure 1). Let $c_i(x, t)$ be the solute concentration [ML^{-3}] in the i th layer, where $x \in (\ell_{i-1}, \ell_i)$ is the distance from the inlet at $x = 0$ and $t > 0$ is time. The governing transport equation in the i th layer is

$$R_i \frac{\partial c_i}{\partial t} = D_i \frac{\partial^2 c_i}{\partial x^2} - v_i \frac{\partial c_i}{\partial x} - \mu_i c_i + \gamma_i, \quad (1)$$

where $R_i > 0$ is the retardation factor $[-]$, $D_i > 0$ is the dispersion coefficient [L^2T^{-1}], v_i is the pore-water velocity [LT^{-1}], μ_i is the rate constant for first-order decay [$\text{ML}^{-3}\text{T}^{-1}$] and γ_i is the rate constant for zero-order production [T^{-1}] (van Genuchten and Alves 1982). Throughout this paper we will denote by $c(x, t)$ the result of amalgamating the layer concentrations, $c_i(x, t)$ ($i = 1, \dots, m$), as defined in Figure 1.

The transport equations (1) are accompanied by initial, interface and boundary conditions. The concentration is initially assumed constant in each layer

$$c_i(x, 0) = f_i, \quad (2)$$

concentration and dispersive flux is assumed continuous at the interfaces between adjacent layers ($i = 1, \dots, m-1$) (Leij et al. 1991; Liu et al. 1998; Guerrero et al. 2013):

$$c_i(\ell_i, t) = c_{i+1}(\ell_i, t), \quad (3)$$

$$\theta_i D_i \frac{\partial c_i}{\partial x}(\ell_i, t) = \theta_{i+1} D_{i+1} \frac{\partial c_{i+1}}{\partial x}(\ell_i, t), \quad (4)$$

and general Robin boundary conditions are considered at the inlet ($x = 0$) and outlet ($x = L$):

$$a_0 c_1(0, t) - b_0 \frac{\partial c_1}{\partial x}(0, t) = g_0(t), \quad (5)$$

$$a_L c_m(L, t) + b_L \frac{\partial c_m}{\partial x}(L, t) = g_L(t). \quad (6)$$

The constant θ_i appearing in the interface condition (4) is the volumetric water content [L^3L^{-3}] in the i th layer (van Genuchten and Alves 1982). In the boundary conditions (5)–(6), a_0 , b_0 , a_L and b_L are constants and $g_0(t)$ and $g_L(t)$ are arbitrary specified functions of time with the subscripts 0 and L denoting the inlet ($x = 0$) and outlet ($x = L$), respectively (Figure 1). We remark that b_0 and b_L are both non-negative, at least one of a_0 or b_0 must be non-zero and at least one of a_L and b_L must be non-zero.

For solute transport problems, commonly (Leij et al. 1991; Liu et al. 1998; Goltz and Huang 2017) either a concentration-type boundary condition

$$c_1(0, t) = c_0(t), \quad (7)$$

or a flux-type boundary condition

$$v_1 c_1(0, t) - D_1 \frac{\partial c_1}{\partial x}(0, t) = v_1 c_0(t), \quad (8)$$

is applied at the inlet, where $c_0(t)$ is the specified inlet concentration, while a zero concentration gradient is applied at the outlet:

$$\frac{\partial c_m}{\partial x}(L, t) = 0. \quad (9)$$

These boundary conditions are obtained from the general boundary conditions (5)–(6) by setting $a_0 = 1$, $b_0 = 0$, $g_0(t) = c_0(t)$ [Eq (7)], $a_0 = v_1$, $b_0 = D_1$, $g_0(t) = v_1 c_0(t)$ [Eq (8)] and $a_L = 0$, $b_L = 1$, $g_L(t) = 0$ [Eq (9)], respectively.

3 Semi-analytical solution

3.1 General solution for m layers in Laplace space

To solve the multilayer transport model (1)–(6), we reformulate the model into m isolated single layer problems (Carr and Turner 2016; Rodrigo and Worthy 2016; Zimmerman et al. 2016). Introducing unknown functions of time, $g_i(t)$ ($i = 1, \dots, m-1$), to denote the following scalar multiple of the (negative) dispersive flux at the layer interfaces (Carr and Turner 2016; Rodrigo and Worthy 2016):

$$g_i(t) = \theta_i D_i \frac{\partial c_i}{\partial x}(\ell_i, t),$$

yields the following equivalent form for the multilayer transport model (1)–(6):

First layer ($i = 1$)

$$R_1 \frac{\partial c_1}{\partial t} = D_1 \frac{\partial^2 c_1}{\partial x^2} - v_1 \frac{\partial c_1}{\partial x} - \mu_1 c_1 + \gamma_1, \quad (10)$$

$$c_1(x, 0) = f_1, \quad (11)$$

$$a_0 c_1(0, t) - b_0 \frac{\partial c_1}{\partial t}(0, t) = g_0(t), \quad (12)$$

$$\theta_1 D_1 \frac{\partial c_1}{\partial x}(\ell_1, t) = g_1(t), \quad (13)$$

Middle layers ($i = 2, \dots, m-1$)

$$R_i \frac{\partial c_i}{\partial t} = D_i \frac{\partial^2 c_i}{\partial x^2} - v_i \frac{\partial c_i}{\partial x} - \mu_i c_i + \gamma_i, \quad (14)$$

$$c_i(x, 0) = f_i, \quad (15)$$

$$\theta_i D_i \frac{\partial c_i}{\partial x}(\ell_{i-1}, t) = g_{i-1}(t), \quad (16)$$

$$\theta_i D_i \frac{\partial c_i}{\partial x}(\ell_i, t) = g_i(t), \quad (17)$$

Last layer ($i = m$)

$$R_m \frac{\partial c_m}{\partial t} = D_m \frac{\partial^2 c_m}{\partial x^2} - v_m \frac{\partial c_m}{\partial x} - \mu_m c_m + \gamma_m, \quad (18)$$

$$c_m(x, 0) = f_m, \quad (19)$$

$$\theta_m D_m \frac{\partial c_m}{\partial x}(\ell_{m-1}, t) = g_{m-1}(t), \quad (20)$$

$$a_L c_m(L, t) + b_L \frac{\partial c_m}{\partial x}(L, t) = g_L(t), \quad (21)$$

with each problem coupled together by imposing continuity of concentration at the interfaces between adjacent layers (3) (Carr and Turner 2016; Rodrigo and Worthy 2016; Carr and March 2018).

We remark that the advection-dispersion-reaction equations (10), (14) and (18) can be reduced to standard heat/diffusion equations via the change of variables:

$$c_i(x, t) = \frac{\gamma_i}{\mu_i} + \exp\left(\frac{v_i x}{2D_i} - \left[\frac{v_i^2}{4R_i D_i} + \frac{\mu_i}{R_i}\right] t\right) u_i(x, t). \quad (22)$$

This seems to suggest that the transformed problem is amenable to solution by methods designed for the multilayer diffusion problem presented in previous work (e.g. Carr and Turner (2016), etc). However, this is not the case as the transformation (22) gives rise to an advection term in the interface conditions (13), (16)–(17) and (20) for the transformed variable $u_i(x, t)$ that would require the solutions to be redeveloped. Moreover, the transformation complicates the problem converting the initial conditions (11), (15), (19) from constants to spatially-dependent. We therefore do not invoke the transformation (22) and take an alternative approach in this paper.

To solve the isolated single-layer problems (10)–(13), (14)–(17) and (18)–(21), we take Laplace transforms yielding the boundary value problems:

First layer ($i = 1$)

$$D_1 C_1'' - v_1 C_1' - (\mu_1 + R_1 s) C_1 = -R_1 f_1 - \frac{\gamma_1}{s}, \quad (23)$$

$$a_0 C_1(0, s) - b_0 C_1'(0, s) = G_0(s), \quad (24)$$

$$\theta_1 D_1 C_1'(\ell_1, s) = G_1(s), \quad (25)$$

Middle layers ($i = 2, \dots, m-1$)

$$D_i C_i'' - v_i C_i' - (\mu_i + R_i s) C_i = -R_i f_i - \frac{\gamma_i}{s}, \quad (26)$$

$$\theta_i D_i C_i'(\ell_{i-1}, s) = G_{i-1}(s), \quad (27)$$

$$\theta_i D_i C_i'(\ell_i, s) = G_i(s), \quad (28)$$

Last layer ($i = m$)

$$D_m C_m'' - v_m C_m' - (\mu_m + R_m s) C_m = -R_m f_m - \frac{\gamma_m}{s}, \quad (29)$$

$$\theta_m D_m C_m'(\ell_{m-1}, s) = G_{m-1}(s), \quad (30)$$

$$a_L C_m(L, s) + b_L C_m'(L, s) = G_L(s), \quad (31)$$

where the prime notation ($'$) denotes a derivative with respect to x , $C_i(x, s) = \mathcal{L}\{c_i(x, t)\}$ denotes the Laplace transform of $c_i(x, t)$ with transformation variable $s \in \mathbb{C}$ and $G_i(s) = \mathcal{L}\{g_i(t)\}$ for $i = 1, \dots, m-1$. Both $G_0(s) = \mathcal{L}\{g_0(t)\}$ and $G_L(s) = \mathcal{L}\{g_L(t)\}$ are assumed to be able to be found analytically. The boundary value problems (23)–(25), (26)–(28) and (29)–(31) all involve second-order constant-coefficient differential equations, which can be solved using standard techniques to give the following expressions for the concentration in the Laplace domain:

$$C_1(x, s) = A_1(x, s)G_0(s) + B_1(x, s)G_1(s) + P_1(x, s), \quad (32)$$

$$C_i(x, s) = A_i(x, s)G_{i-1}(s) + B_i(x, s)G_i(s) + P_i(x, s), \quad i = 2, \dots, m-1, \quad (33)$$

$$C_m(x, s) = A_m(x, s)G_{m-1}(s) + B_m(x, s)G_L(s) + P_m(x, s), \quad (34)$$

where the functions P_i , A_i and B_i ($i = 1, \dots, m$) are defined in Table 1.

With all other variables in the expressions (32)–(34) defined, to determine $G_1(s), \dots, G_{m-1}(s)$, the Laplace transformations of the unknown interface functions $g_1(t), \dots, g_{m-1}(t)$, we enforce continuity of concentration (3) at each interface in the Laplace domain (Carr and Turner 2016; Rodrigo and Worthy 2016; Carr and March 2018):

$$C_i(\ell_i, s) = C_{i+1}(\ell_i, s), \quad i = 1, \dots, m-1. \quad (35)$$

Table 1 Definition of the functions $P_i(x, s)$, $A_i(x, s)$ and $B_i(x, s)$ ($i = 1, \dots, m$) appearing in the Laplace domain concentrations (32)–(34).

<p>First layer ($i = 1$)</p> $P_1(x, s) = \Psi_1(s) + \frac{a_0}{\beta_1(s)} \left\{ \lambda_{1,1}(s) \Psi_{1,2}(x, s) - \lambda_{1,2}(s) \Psi_{1,2}(\ell_1, s) \Psi_{1,1}(x, s) \right\} \Psi_1(s),$ $A_1(x, s) = \frac{1}{\beta_1(s)} \left\{ \lambda_{1,2}(s) \Psi_{1,2}(\ell_1, s) \Psi_{1,1}(x, s) - \lambda_{1,1}(s) \Psi_{1,2}(x, s) \right\},$ $B_1(x, s) = \frac{1}{\theta_1 D_1 \beta_1(s)} \left\{ [a_0 - b_0 \lambda_{1,1}(s)] \Psi_{1,1}(0, s) \Psi_{1,2}(x, s) - [a_0 - b_0 \lambda_{1,2}(s)] \Psi_{1,1}(x, s) \right\},$ <p>where</p> $\beta_1(s) = [a_0 - b_0 \lambda_{1,1}(s)] \lambda_{1,2}(s) \exp(-[\lambda_{1,1}(s) - \lambda_{1,2}(s)] \ell_1) - [a_0 - b_0 \lambda_{1,2}(s)] \lambda_{1,1}(s).$
<p>Middle layers ($i = 2, \dots, m-1$)</p> $P_i(x, s) = \Psi_i(s),$ $A_i(x, s) = \frac{1}{\theta_i D_i \beta_i(s)} \left\{ \lambda_{i,2}(s) \Psi_{i,2}(\ell_i, s) \Psi_{i,1}(x, s) - \lambda_{i,1}(s) \Psi_{i,2}(x, s) \right\},$ $B_i(x, s) = \frac{1}{\theta_i D_i \beta_i(s)} \left\{ \lambda_{i,1}(s) \Psi_{i,1}(\ell_{i-1}, s) \Psi_{i,2}(x, s) - \lambda_{i,2}(s) \Psi_{i,1}(x, s) \right\},$ <p>where</p> $\beta_i(s) = \lambda_{i,1}(s) \lambda_{i,2}(s) \left\{ \exp(-[\lambda_{i,1}(s) - \lambda_{i,2}(s)](\ell_i - \ell_{i-1})) - 1 \right\}.$
<p>Last layer ($i = m$)</p> $P_m(x, s) = \Psi_m(s) + \frac{a_L}{\beta_m(s)} \left\{ \lambda_{m,2}(s) \Psi_{m,1}(x, s) - \lambda_{m,1}(s) \Psi_{m,1}(\ell_{m-1}, s) \Psi_{m,2}(x, s) \right\} \Psi_m(s),$ $A_m(x, s) = \frac{1}{\theta_m D_m \beta_m(s)} \left\{ [a_L + b_L \lambda_{m,2}(s)] \Psi_{m,2}(L, s) \Psi_{m,1}(x, s) - [a_L + b_L \lambda_{m,1}(s)] \Psi_{m,2}(x, s) \right\},$ $B_m(x, s) = \frac{1}{\beta_m(s)} \left\{ \lambda_{m,1}(s) \Psi_{m,1}(\ell_{m-1}, s) \Psi_{m,2}(x, s) - \lambda_{m,2}(s) \Psi_{m,1}(x, s) \right\},$ <p>where</p> $\beta_m(s) = [a_L + b_L \lambda_{m,2}(s)] \lambda_{m,1}(s) \exp(-[\lambda_{m,1}(s) - \lambda_{m,2}(s)](\ell_m - \ell_{m-1})) - [a_L + b_L \lambda_{m,1}(s)] \lambda_{m,2}(s).$ <p>For all layers ($i = 1, \dots, m$):</p> $\Psi_i(s) = \frac{\gamma_i s^{-1} + R_i f_i}{\mu_i + R_i s},$ $\Psi_{i,1}(x, s) = \exp[\lambda_{i,1}(s)(x - \ell_i)] \text{ recalling } \ell_m = L,$ $\Psi_{i,2}(x, s) = \exp[\lambda_{i,2}(s)(x - \ell_{i-1})] \text{ recalling } \ell_0 = 0,$ $\lambda_{i,1}(s) = \frac{v_i + \sqrt{v_i^2 + 4D_i(R_i s + \mu_i)}}{2D_i},$ $\lambda_{i,2}(s) = \frac{v_i - \sqrt{v_i^2 + 4D_i(R_i s + \mu_i)}}{2D_i}.$

Substituting (32)–(34) into the system of equations (35) yields a linear system for $\mathbf{x} = [G_1(s), \dots, G_{m-1}(s)]^T$, expressible in matrix form as

$$\mathbf{Ax} = \mathbf{b}, \tag{36}$$

where $\mathbf{A} = (a_{i,j}) \in \mathbb{C}^{(m-1) \times (m-1)}$ is a tridiagonal matrix and $\mathbf{b} = (b_i) \in \mathbb{C}^{(m-1)}$ is a vector with entries:

$$\begin{aligned} a_{1,1} &= B_1(\ell_1, s) - A_2(\ell_1, s), \\ a_{1,2} &= -B_2(\ell_1, s), \\ a_{i,i-1} &= A_i(\ell_i, s), \quad i = 2, \dots, m-2, \\ a_{i,i} &= B_i(\ell_i, s) - A_{i+1}(\ell_i, s), \quad i = 2, \dots, m-2, \\ a_{i,i+1} &= -B_{i+1}(\ell_i, s), \quad i = 2, \dots, m-2, \\ a_{m-1,m-2} &= A_{m-1}(\ell_{m-1}, s), \\ a_{m-1,m-1} &= B_{m-1}(\ell_{m-1}, s) - A_m(\ell_{m-1}, s), \\ b_1 &= P_2(\ell_1, s) - P_1(\ell_1, s) - A_1(\ell_1, s)G_0(s), \\ b_i &= P_{i+1}(\ell_i, s) - P_i(\ell_i, s), \quad i = 2, \dots, m-2, \\ b_{m-1} &= P_m(\ell_{m-1}, s) - P_{m-1}(\ell_{m-1}, s) + B_m(\ell_{m-1}, s)G_L(s). \end{aligned}$$

Solving the linear system (36) allows the functions $G_1(s), \dots, G_{m-1}(s)$ to be computed and hence the Laplace transform of the concentration (32)–(34) can be evaluated at any x and s in the Laplace domain.

3.2 Simplification for two layers in Laplace space

The formulation presented in the previous section breaks down for $m = 2$ layers due to the assumption of middle layers. While the expressions for $C_1(x, s)$ (32) and $C_2(x, s)$ (34) remain valid:

$$\begin{aligned} C_1(x, s) &= A_1(x, s)G_0(s) + B_1(x, s)G_1(s) + P_1(x, s), \\ C_2(x, s) &= A_2(x, s)G_1(s) + B_2(x, s)G_L(s) + P_2(x, s), \end{aligned}$$

the defined entries of the linear system (36) are no longer valid for $m = 2$. In this case, the linear system (36) reduces to a single equation that can be solved to yield:

$$G_1(s) = (B_1(\ell_1, s) - A_2(\ell_1, s))^{-1} [P_2(\ell_1, s) - P_1(\ell_1, s) - A_1(\ell_1, s)G_0(s) + B_2(\ell_1, s)G_L(s)],$$

which allows $C_1(x, s)$ and $C_2(x, s)$ to be evaluated at any x and s .

3.3 Numerical inversion of Laplace transform

To convert the Laplace domain expressions (32)–(34) back to the time domain and thereby obtain the concentration $c_i(x, t)$ ($i = 1, \dots, m$), we need to compute the inverse Laplace transform:

$$c_i(x, t) = \mathcal{L}^{-1} \{C_i(x, s)\} = \frac{1}{2\pi i} \int_{\Gamma} e^{st} C_i(x, s) ds,$$

where Γ is a Hankel contour that begins at $-\infty - 0i$, winds around the origin and terminates at $-\infty + 0i$ (Trefethen et al. 2006). Introducing the change of variable $z = st$, using a rational approximation to e^z and applying residue calculus (see Trefethen et al. (2006) for full details) yields the numerical inversion formula:

$$c_i(x, t) = \mathcal{L}^{-1} \{C_i(x, s)\} \approx -\frac{2}{t} \Re \left\{ \sum_{k \in \mathbb{O}_N} w_k C_i(x, s_k) \right\}, \quad (37)$$

where N is even, \mathbb{O}_N is the set of positive odd integers less than N , $s_k = z_k/t$ and $w_k, z_k \in \mathbb{C}$ are the residues and poles of the best (N, N) rational approximation to e^z on the negative real line. Both w_k and z_k are constants, which are independent of x and t and computed using a supplied MATLAB function (Trefethen et al. 2006, Fig 4.1).

3.4 Treatment of step function boundary conditions

Suppose the inlet concentration $c_0(t)$ in either the concentration-type (7) or flux type (8) boundary condition, is a Heaviside step function of duration $t_0 > 0$:

$$c_0(t) = c_0 H(t_0 - t) = \begin{cases} c_0, & 0 < t < t_0, \\ 0, & t > t_0, \end{cases}$$

where c_0 is a constant. In solute transport problems, such boundary conditions are commonly (van Genuchten and Alves 1982; Leij et al. 1991; Goltz and Huang 2017) paired with a zero concentration gradient at the outlet (9) and lead to $G_0(s) = \exp(-t_0 s)/s$ and $G_0(s) = v_1 \exp(-t_0 s)/s$ in Eq (32) for the concentration-type and flux-type boundary condition, respectively. Such exponential functions are well known to cause numerical problems in algorithms for inverting Laplace transforms (Kuhlman 2013). The approximation (37) indeed suffers from this issue as evaluating $\exp(-t_0 s)$ at $s = s_k = z_k/t$ for poles z_k with negative real part leads to floating point overflow for small t . To overcome this problem, we use superposition of solutions. Consider, for example, the multilayer transport model (1)–(4) subject to the boundary conditions (7) or (8), and (9). The solution to this problem can be expressed as

$$c_i(x, t) = \begin{cases} \tilde{c}_i(x, t), & 0 < t < t_0, \\ \tilde{c}_i(x, t) - \hat{c}_i(x, t - t_0), & t > t_0, \end{cases}$$

where $\tilde{c}_i(x, t)$ is the solution of the multilayer transport model (1)–(6) with $g_0(t) = c_0$ and $\hat{c}_i(x, t)$ is the solution of the multilayer transport model (1)–(6) with $g_0(t) = c_0$, $f_i = 0$ and $\gamma_i = 0$. Both $\tilde{c}_i(x, t)$ and $\hat{c}_i(x, t)$ are obtained using the approach outlined in subsections 3.1–3.3.

4 Results

We now demonstrate application of our semi-analytical Laplace-transform solution and verify that it produces the correct results using a selection of test cases. The transport parameters, initial conditions and boundary conditions for each problem are provided in Tables 2 and 3. A MATLAB code implementing our semi-analytical solution and producing the results in this section is available for download from github.com/elliottcarr/Carr2020a.

4.1 One and two layer test cases

Cases 1–4 consider advection-dispersion-reaction in a homogeneous (single-layer) medium of length 30 cm. The concentration is initially zero everywhere and a zero concentration gradient is applied at the outlet (9). Four different boundary conditions are considered at the inlet:

- Case 1: flux-type boundary condition (8) with constant inlet concentration $c_0(t) = c_0$;
- Case 2: flux-type boundary condition (8) with step inlet concentration $c_0(t) = c_0 H(t_0 - t)$ and pulse duration $t_0 = 0.5$ days;
- Case 3: concentration-type boundary condition (7) with constant inlet concentration $c_0(t) = c_0$;
- Case 4: concentration-type boundary condition (7) with step inlet concentration $c_0(t) = c_0 H(t_0 - t)$ and pulse duration $t_0 = 0.5$ days.

To solve these single-layer problems using our semi-analytical method, we choose $m = 2$ layers and set the transport parameters equal in both layers (see Table 2). In Table 4, the relative concentration distributions ($c(x, t)/c_0$) obtained are compared to corresponding distributions obtained using analytical solutions given in the literature (van Genuchten and Alves 1982, sections C7 and C8), which are valid for homogeneous (single-layer) media only. For all four problems, the maximum absolute difference between the relative concentration distributions obtained using both solution methods is tabulated in Table 4 at $t = 10^{-3}, 0.1, 0.6, 1, 2, 4$ days. These results demonstrate that both solutions are in excellent agreement for each choice of inlet condition and verify that our semi-analytical solution produces the correct results for single-layer media.

Next, we present results for three two-layer test cases that have frequently appeared in the literature (Leij and van Genuchten 1995; Liu et al. 1998; Guerrero et al. 2013). The three test cases, labelled cases 5–7, consider advection-dispersion (without decay or production) in a medium of length 30 cm with first and second layers

Table 2 Transport parameters, geometry and initial conditions for the various test cases, where i is the layer index and ℓ_i locates the end of layer i [cm]. In the i th layer: R_i is the retardation factor $[-]$, D_i is the dispersion coefficient [$\text{cm}^2\text{day}^{-1}$], v_i is the pore-water velocity [cm day^{-1}], μ_i is the rate constant for first-order decay [day^{-1}], γ_i is the rate constant for zero-order production [$\text{kg cm}^{-3}\text{ day}^{-1}$], θ_i is the volumetric water content $[-]$ and f_i is the initial constant concentration [kg cm^{-3}]. Dashed horizontal lines for case 12 indicate the artificial layer created to accommodate the injected contaminant initial condition (see section 4).

Case	i	ℓ_i	R_i	D_i	v_i	μ_i	γ_i	θ_i	f_i
1–4	1	10	1	50	75	2	1	0.4	0
	2	30	1	50	75	2	1	0.4	0
5	1	10	1	50	25	0	0	0.4	0
	2	30	1	20	40	0	0	0.25	0
6	1	10	1	50	25	0	0	0.4	0
	2	30	1	20	40	0	0	0.25	0
7	1	10	1	50	25	0	0	0.4	0
	2	30	1	20	40	0	0	0.25	0
8	1	10	3	50	25	3	0	0.4	0
	2	20	2	20	40	4	0	0.25	0
9-10, 11	1	10	4.25	7	10	0	0	0.4	0
	2	12	14	18	8	0	0	0.5	0
	3	20	4.25	7	10	0	0	0.4	0
	4	22	14	18	8	0	0	0.5	0
	5	30	4.25	7	10	0	0	0.4	0
12	1	10	4.25	7	10	0	0	0.4	0
	2	12	14	18	8	0	0	0.5	0
	3	14	4.25	7	10	0	0	0.4	0
	4	18	4.25	7	10	0	0	0.4	c_0
	5	20	4.25	7	10	0	0	0.4	0
	6	22	14	18	8	0	0	0.5	0
	7	30	4.25	7	10	0	0	0.4	0
13	1	10	4.25	7	10	3	2	0.4	0
	2	12	14	18	8	2	4	0.5	0
	3	20	4.25	7	10	3	2	0.4	0
	4	22	14	18	8	2	4	0.5	c_0
	5	30	4.25	7	10	3	2	0.4	0

Table 3 Choice of inlet boundary condition (5) for the various test cases. For all test cases, a zero concentration gradient is assumed at the outlet with parameters $a_L = 0$, $b_L = 1$ and $g_L(t) = 0$ specified in the outlet boundary condition (6).

Case	a_0	b_0	$g_0(t)$
1, 5–9	v_1	D_1	$v_1 c_0$
2, 10, 13	v_1	D_1	$v_1 c_0 H(t_0 - t)$
3	1	0	c_0
4	1	0	$c_0 H(t_0 - t)$
11	1	0	$c_0 \alpha t e^{-\beta t}$
12	0	1	0

Table 4 Comparison between our semi-analytical Laplace transform solution (see section 3) and the analytical solutions catalogued in van Genuchten and Alves (1982) for the homogeneous medium test cases (1–4). The tabulated values are the maximum absolute difference between the values of the relative concentration ($c(x, t)/c_0$) computed using the two approaches over the discrete range $x = 0, 2, \dots, 20$ cm, with $N = 14$ poles/residues used for numerically inverting the Laplace transform (37). As recommended by van Genuchten and Alves (1982), if $v_1 L/D_1 > \min(5 + 40v_1 t/(R_1 L), 5 + 40v_1(t - t_0)/(R_1 L), 100)$, the analytical solution is calculated using the approximate solutions catalogued (van Genuchten and Alves 1982). Otherwise the eigenfunction expansion solutions are used with 1000 eigenvalues/terms taken in the series expansions (see van Genuchten and Alves (1982) and our code for full details).

Case	$t = 10^{-3}$	$t = 0.1$	$t = 0.6$	$t = 1$	$t = 2$	$t = 4$
1	4.11×10^{-14}	5.53×10^{-10}	5.84×10^{-8}	9.38×10^{-9}	4.75×10^{-9}	6.10×10^{-10}
2	4.11×10^{-14}	5.53×10^{-10}	1.89×10^{-8}	7.10×10^{-8}	1.74×10^{-8}	5.90×10^{-10}
3	1.98×10^{-14}	7.61×10^{-10}	1.93×10^{-8}	1.53×10^{-8}	1.20×10^{-9}	3.34×10^{-10}
4	1.98×10^{-14}	7.61×10^{-10}	1.93×10^{-8}	1.57×10^{-9}	1.15×10^{-8}	8.10×10^{-10}

Table 5 Relative concentration values ($c(x, t)/c_0$) for test cases 5–7 computed using our semi-analytical Laplace transform (SALT) solution (see section 3) with $N = 14$ poles/residues used in the numerical inversion of the Laplace transform (37). Results are compared with previously published values given by Guerrero, Pimentel, and Skaggs (2013) (GPS), Liu, Ball, and Ellis (1998) (LBE) and Leij and van Genuchten (1995) (LVG). Shaded cells highlight discrepancies between the different methods by indicating when one of the four computed values differs from the others.

Case	x	$t = 0.2$				$t = 0.4$				$t = 0.6$				$t = 0.8$			
		SALT	GPS	LBE	LVG	SALT	GPS	LBE	LVG	SALT	GPS	LBE	LVG	SALT	GPS	LBE	LVG
5	0	0.884	0.884	0.884	0.884	0.963	0.963	0.963	0.963	0.987	0.987	0.987	0.987	0.995	0.995	0.995	0.995
	2	0.742	0.742	0.742	0.742	0.915	0.915	0.915	0.915	0.969	0.969	0.969	0.969	0.988	0.988	0.988	0.988
	4	0.561	0.561	0.561	0.561	0.841	0.841	0.841	0.841	0.940	0.940	0.940	0.940	0.977	0.977	0.977	0.977
	6	0.375	0.375	0.374	0.375	0.746	0.746	0.746	0.746	0.901	0.901	0.901	0.901	0.962	0.962	0.962	0.962
	8	0.222	0.222	0.222	0.222	0.645	0.645	0.645	0.645	0.858	0.858	0.858	0.858	0.945	0.945	0.945	0.945
	10	0.142	0.142	0.142	0.142	0.579	0.579	0.579	0.579	0.829	0.829	0.829	0.829	0.933	0.933	0.933	0.933
	12	0.063	0.063	0.063	0.063	0.480	0.480	0.480	0.480	0.781	0.781	0.781	0.781	0.914	0.914	0.914	0.914
	14	0.021	0.021	0.021	0.021	0.372	0.372	0.372	0.372	0.722	0.722	0.722	0.722	0.889	0.889	0.889	0.889
	16	0.005	0.005	0.005	0.005	0.264	0.264	0.265	0.264	0.651	0.651	0.651	0.651	0.858	0.858	0.858	0.858
	18	0.001	0.001	0.001	0.001	0.168	0.168	0.169	0.168	0.567	0.567	0.567	0.567	0.819	0.819	0.819	0.819
	20	0.000	0.000	0.000	0.000	0.094	0.094	0.094	0.094	0.473	0.473	0.473	0.473	0.770	0.770	0.770	0.770
6	0	0.978	0.978	0.977	0.978	0.998	0.998	0.998	0.998	1.000	1.000	1.000	1.000	1.000	1.000	1.000	1.000
	2	0.868	0.868	0.867	0.868	0.984	0.984	0.984	0.984	0.998	0.998	0.998	0.998	1.000	1.000	1.000	1.000
	4	0.634	0.634	0.633	0.634	0.942	0.942	0.942	0.942	0.991	0.991	0.991	0.991	0.999	0.999	0.999	0.999
	6	0.345	0.345	0.345	0.345	0.849	0.849	0.849	0.849	0.972	0.972	0.972	0.972	0.995	0.995	0.995	0.995
	8	0.131	0.131	0.131	0.131	0.693	0.693	0.693	0.693	0.930	0.930	0.929	0.930	0.986	0.986	0.986	0.986
	10	0.033	0.033	0.033	0.033	0.496	0.496	0.496	0.496	0.853	0.853	0.853	0.853	0.966	0.966	0.966	0.966
	12	0.011	0.011	0.011	0.011	0.370	0.370	0.370	0.370	0.784	0.784	0.783	0.784	0.944	0.944	0.944	0.944
	14	0.003	0.003	0.003	0.003	0.257	0.257	0.257	0.257	0.699	0.699	0.698	0.699	0.913	0.913	0.913	0.913
	16	0.001	0.001	0.001	0.001	0.166	0.166	0.166	0.166	0.601	0.601	0.601	0.601	0.871	0.871	0.871	0.871
	18	0.000	0.000	0.000	0.000	0.098	0.098	0.099	0.098	0.498	0.498	0.498	0.498	0.817	0.817	0.817	0.817
	20	0.000	0.000	0.000	0.000	0.054	0.054	0.054	0.054	0.395	0.395	0.395	0.395	0.751	0.751	0.750	0.751
7	0	0.999	0.999	0.999	0.999	1.000	1.000	1.000	1.000	1.000	1.000	1.000	1.000	1.000	1.000	1.000	1.000
	2	0.988	0.988	0.987	0.988	1.000	1.000	1.000	1.000	1.000	1.000	1.000	1.000	1.000	1.000	1.000	1.000
	4	0.928	0.928	0.928	0.928	0.999	0.999	0.999	0.999	1.000	1.000	1.000	1.000	1.000	1.000	1.000	1.000
	6	0.764	0.764	0.763	0.764	0.995	0.995	0.995	0.995	1.000	1.000	1.000	1.000	1.000	1.000	1.000	1.000
	8	0.496	0.496	0.495	0.496	0.976	0.976	0.976	0.976	0.998	0.998	0.998	0.998	0.999	0.999	0.999	0.999
	10	0.152	0.152	0.152	0.152	0.780	0.780	0.779	0.780	0.940	0.940	0.939	0.940	0.979	0.979	0.978	0.979
	12	0.049	0.049	0.050	0.049	0.600	0.600	0.600	0.600	0.870	0.870	0.870	0.870	0.952	0.952	0.952	0.952
	14	0.013	0.013	0.013	0.013	0.418	0.418	0.418	0.417	0.773	0.773	0.773	0.773	0.911	0.911	0.910	0.911
	16	0.003	0.003	0.003	0.003	0.262	0.262	0.262	0.262	0.653	0.653	0.653	0.653	0.851	0.851	0.851	0.851
	18	0.000	0.000	0.000	0.000	0.148	0.148	0.148	0.148	0.522	0.522	0.522	0.522	0.774	0.774	0.774	0.774
	20	0.000	0.000	0.000	0.000	0.075	0.075	0.075	0.075	0.393	0.393	0.393	0.393	0.681	0.681	0.681	0.681

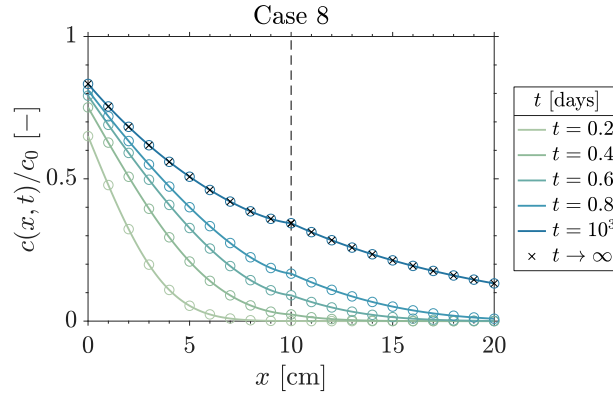


Fig. 2 Relative concentration spatial profiles ($c(x, t)/c_0$) over time for test case 8. Continuous lines indicate our semi-analytical Laplace transform solution (see section 3) with $N = 14$ poles/residues used in the numerical inversion of the Laplace transform (37). Circle markers indicate the numerical solution obtained using the finite volume scheme outlined in Appendix A computed with $n = 601$ nodes but plotted with markers at $x = 0, 1, \dots, 20$ cm only. Crosses indicate the exact steady-state solution obtained by solving the steady-state analogue of the multilayer transport model (1)–(6) analytically. The vertical dashed line indicates the location of the interface at $x = 10$ cm. The plot is truncated at $x = 20$ cm rather than shown for the full length of the medium ($x = 30$ cm) inline with Guerrero et al. (2013).

of length 10 cm and 20 cm, respectively. A constant flux-type boundary condition is applied at the inlet (Eq (8) with $c_0(t) = c_0$) and a zero concentration gradient is applied at the outlet (9). Initially, the concentration is assumed to be zero in both layers. Different transport parameter combinations are applied for the three test cases (see Table 2). In Table 5, for all three test cases, we report the relative concentration values obtained from our semi-analytical solution at several equidistant points in space and time. These results are compared to those previously reported by Guerrero et al. (2013), Liu et al. (1998) and Leij and van Genuchten (1995) with all numerical values in Table 5 displayed to three decimal places to be consistent with the numerical values reported in those papers. For all three test cases, our results agree precisely with those of Guerrero et al. (2013) to the precision reported. When compared to Liu et al. (1998) and Leij and van Genuchten (1995), minor

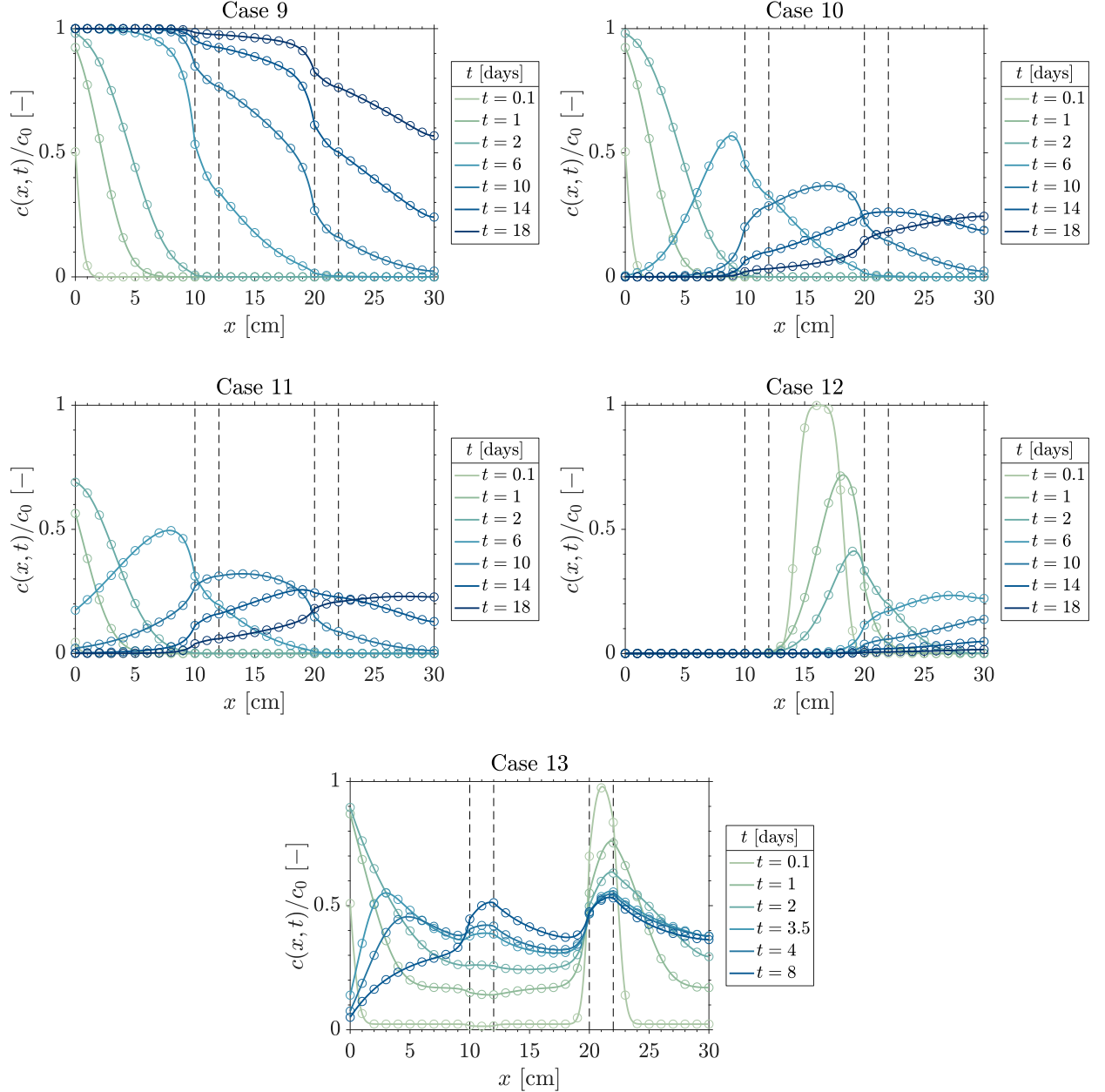


Fig. 3 Relative concentration spatial profiles ($c(x, t)/c_0$) over time for test cases 9–13. Continuous lines indicate our semi-analytical Laplace transform solution (see section 3) with $N = 14$ poles/residues used in the numerical inversion of the Laplace transform (37). Circle markers indicate the numerical solution obtained using the finite volume scheme outlined in Appendix A computed with $n = 601$ nodes but plotted with markers at $x = 0, 1, \dots, 30$ cm only. Vertical dashed lines indicate the location of the layer interfaces at $x = 10, 12, 20, 22$ cm.

differences of ± 0.001 are evident as highlighted in Table 5. These discrepancies are likely to be explained by [Leij and van Genuchten \(1995\)](#) considering a semi-infinite second layer and using a different method for numerically inverting the Laplace transform and [Liu et al. \(1998\)](#) considering a finite second layer of undisclosed length.

Lastly, we present results for a final two-layer test case previously considered by [Guerrero et al. \(2013\)](#). This problem, labelled case 8, is the same as case 6 with the exception that first-order decay is present in both layers (see Table 2). In Figure 2, we plot the relative concentration distributions obtained from our semi-analytical solution at $t = 0.2, 0.4, 0.6, 0.8$ days (as in [Guerrero et al. \(2013\)](#)) and $t = 10^3$ when the solution is visible indistinguishable from its steady state. At short time, our results match well with [Guerrero et al. \(2013\)](#)'s results but differ for long times and at steady-state. However, agreement with the numerical solution (outlined in Appendix A) as well as the exact steady-state solution obtained by solving the steady-state analogue of the multilayer transport model (1)–(6) (see Figure 2) supports that our approach produces the correct results.

4.2 Multiple layer test cases

We now apply our semi-analytical solution to some test cases involving five or more layers. Our solutions are compared to previously reported results from the literature and/or numerical solutions obtained using a finite volume method, briefly discussed in Appendix A.

Firstly, we consider the five-layer test case previously considered by [Liu et al. \(1998\)](#) and [Guerrero et al. \(2013\)](#). This test case involves advection-dispersion (without decay or production) in a medium of length 30 cm consisting of alternating layers of sand–clay–sand–clay–sand (cases 9–10 in Tables 2 and 3). The initial concentration is zero in each layer and a zero concentration gradient is applied at the outlet. Two different boundary conditions are considered at the inlet:

- Case 9: flux-type boundary condition (8) with constant inlet concentration $c_0(t) = c_0$;
- Case 10: flux-type boundary condition (8) with step inlet concentration $c_0(t) = c_0 H(t_0 - t)$ and pulse duration $t_0 = 3$ days.

In Figure 3, we plot the relative concentration distributions ($c(x, t)/c_0$) obtained from our semi-analytical solution at several points in time. Only case 9 is considered by [Liu et al. \(1998\)](#) and [Guerrero et al. \(2013\)](#) who both report relative concentration distributions at $t = 2, 6, 10$ days only with their solutions at these times all in excellent agreement with those for case 9 in Figure 3. For case 10 and the remaining times for case 9, agreement with the relative concentration distributions computed using the numerical method discussed in Appendix A demonstrates that our semi-analytical solution produces the correct results.

To further highlight the capability of our approach, we consider three final test cases (cases 11–13 in Tables 2 and 3). Case 11 is case 9 with a continuously varying inlet concentration (see Table 3). Case 12 considers the same five-layer medium as cases 9–11 but with a zero concentration gradient applied at both the inlet and outlet and an initial condition modelling injection of a contaminant into the medium at time $t = 0$ between $x = 14$ cm and $x = 18$ cm ([Goltz and Huang 2017](#)). This test case is solved by creating an artificial layer extending from $x = 14$ cm to $x = 18$ cm having the same transport parameters as the sand layer in which it is located, leading to a seven-layer formulation as described in Table 2. Finally, case 13 demonstrates the full capability of our semi-analytical solution with non-zero rate constants of decay and production in each layer and multiple contaminant sources (see Tables 2 and 3). The agreement with the relative concentration distributions obtained using the numerical method evident in Figure 3 for cases 11–13 further confirm the correctness of our semi-analytical solution approach.

5 Conclusion

In this paper, we have developed a semi-analytical Laplace-transform based method to solve the one-dimensional linear advection-dispersion-reaction equation in a layered medium. The novelty of the approach is to introduce unknown functions at the interfaces between adjacent layers, which allows the multilayer problem to be isolated and solved separately on each layer before being numerically inverted back to the time domain. Our derived solution is quite general in that it can be applied to problems involving an arbitrary number of layers and arbitrary time-varying boundary conditions at the inlet and outlet. The derived solutions extend and generalise recent work on diffusion ([Carr and Turner 2016](#); [Carr and March 2018](#); [Rodrigo and Worthy 2016](#)) and reaction-diffusion ([Zimmerman et al. 2016](#)) in layered media.

The solutions presented in this paper, and our MATLAB code, are limited to constant initial conditions in each layer and interface conditions imposing continuity of concentration and dispersive flux between adjacent layers. However, extension to other interface conditions that do not impose continuity of concentration (see, e.g., Carr and March (2018)), is straightforward and achieved in our formulation by replacing Eq (35) with the Laplace transform of the imposed condition. For example, solving the multilayer transport model (1)–(6) with concentration continuity (3) replaced by the *partition interface condition* (Carr and March 2018; Carr and Pontrelli 2018), $c_i(\ell_i, t) = \alpha_i c_{i+1}(\ell_i, t)$ where $\alpha_i > 0$ is a specified constant, simply requires replacement of Eq (35) with $C_i(\ell_i, s) = \alpha_i C_{i+1}(\ell_i, s)$ and ultimately a small modification to the entries of the linear system (36). Treatment of spatially-varying initial conditions, where f_i is now $f_i(x)$ in the boundary value problems (23)–(25), (26)–(28) and (29)–(31), is more challenging but possible and would lead to more complicated expressions for the Laplace domain concentration than those defined in Eqs (32)–(34) and Table 1. The method for inverting the Laplace transform can lead to unreliable results for advection-dominated transport so addressing this limitation would be valuable to pursue in the future. Another possible avenue for future research is to extend the semi-analytical solutions to accommodate multispecies transport and/or rate-limited sorption, as described by Chen et al. (2019a,b) for single-layer media and Miele and Zhan (2012) and Chen et al. (2018) for two-layer media. We address the case of multispecies multilayer transport in a forthcoming paper (Carr 2020).

A Numerical solution

In this appendix, we briefly outline the finite volume scheme used to obtain a numerical solution to the multilayer transport model (1)–(6), as mentioned in section 4.

The interval $[0, L]$ is discretised using a uniform grid consisting of n nodes with the k th node located at $x = (k-1)h =: x_k$, where $k = 1, \dots, n$ and $h = L/(n-1)$. The number of nodes n is chosen to ensure that a node coincides with each interface ($x = \ell_i$, $i = 1, \dots, m-1$). Let $\bar{c}_k(t)$ denote the numerical approximation to $c(x, t)$ at $x = x_k$ and

$$\begin{aligned} J_{i,k} &= D_i \frac{\bar{c}_k - \bar{c}_{k-1}}{h} - v_i \frac{\bar{c}_{k-1} + \bar{c}_k}{2}, \\ S_{i,k} &= -\mu_i \bar{c}_k + \gamma_i. \end{aligned}$$

The discrete system takes the form:

$$\mathbf{M} \frac{d\mathbf{c}}{dt} = \mathbf{F}(\mathbf{c}), \quad \mathbf{c}(0) = \mathbf{c}_0, \quad (38)$$

where $\mathbf{M} \in \mathbb{R}^{n \times n}$, $\mathbf{c} = (\bar{c}_1, \dots, \bar{c}_n)^T \in \mathbb{R}^n$ and $\mathbf{F} = (F_1, \dots, F_n)^T \in \mathbb{R}^n$. The initial solution vector $\mathbf{c}_0 \in \mathbb{R}^n$ gets its entries from the initial condition (2) with first entry f_1 , last entry f_m and k th entry ($k = 2, \dots, n-1$) equal to f_i if $x_k \in (\ell_{i-1}, \ell_i)$ or $(f_i + f_{i+1})/2$ if $x_k = \ell_i$, where $i = 1, \dots, m-1$ is the interface index. The form of \mathbf{M} depends on the choice of boundary conditions at the inlet and outlet:

$$\mathbf{M} = \begin{cases} \mathbf{I}, & \text{if } b_0 \neq 0 \text{ and } b_L \neq 0, \\ \mathbf{I} - \mathbf{e}_1 \mathbf{e}_1^T, & \text{if } b_0 = 0 \text{ and } b_L \neq 0, \\ \mathbf{I} - \mathbf{e}_n \mathbf{e}_n^T, & \text{if } b_0 \neq 0 \text{ and } b_L = 0, \\ \mathbf{I} - \mathbf{e}_1 \mathbf{e}_1^T - \mathbf{e}_n \mathbf{e}_n^T, & \text{if } b_0 = 0 \text{ and } b_L = 0, \end{cases}$$

where \mathbf{I} is the $n \times n$ identity matrix and \mathbf{e}_k is the k th column of \mathbf{I} . The components of \mathbf{F} are defined as follows:

$$F_1 = a_0 \bar{c}_1 - g_0(t)$$

if $b_0 = 0$,

$$F_1 = \frac{J_{1,2} + \frac{D_1}{b_0} g_0(t) + (v_1 - D_1 \frac{a_0}{b_0}) \bar{c}_1 + \frac{h}{2} S_{1,1}}{\frac{h}{2} R_1}$$

if $b_0 \neq 0$,

$$F_k = \frac{J_{i,k+1} - J_{i,k} + h S_{i,k}}{h R_i}$$

if $x_k \in (\ell_{i-1}, \ell_i)$,

$$F_k = \frac{\theta_{i+1} J_{i+1,k+1} - \theta_i J_{i,k} + \frac{h}{2} (\theta_i S_{i,k} + \theta_{i+1} S_{i+1,k})}{\frac{h}{2} (\theta_i R_i + \theta_{i+1} R_{i+1})}$$

if $x_k = \ell_i$ and $i = 2, \dots, m-1$,

$$F_n = a_L \bar{c}_n - g_L(t)$$

if $b_L = 0$, and

$$F_n = \frac{\frac{D_m}{b_L} g_L(t) - (v_m + D_m \frac{a_L}{b_L}) \bar{c}_n - J_{m,n} + \frac{h}{2} S_{m,n}}{\frac{h}{2} R_m}$$

if $b_L \neq 0$. The initial value problem (38) is solved using MATLAB's in-built `ode15s` solver with the default tolerances and options of `Mass = M` and `MassSingular = true` if b_0 and/or b_L are zero. The interval of integration (`tspan`) is chosen to return the solution at the appropriate times shown in Figures 2–3.

Acknowledgements This research was funded by the Australian Research Council (DE150101137). We thank the two anonymous reviewers for suggestions that improved the final manuscript.

References

- Carr EJ (2020) Generalized semi-analytical solution for coupled multispecies advection-dispersion equations in multilayer porous media. [arXiv:2006.15793](https://arxiv.org/abs/2006.15793)
- Carr EJ, March NG (2018) Semi-analytical solution of multilayer diffusion problems with time-varying boundary conditions and general interface conditions. *Appl Math Comput* 333:286–303
- Carr EJ, Pontrelli G (2018) Modelling mass diffusion for a multi-layer sphere immersed in a semi-infinite medium: application to drug delivery. *Math Biosci* 303:1–9
- Carr EJ, Turner IW (2016) A semi-analytical solution for multilayer diffusion in a composite medium consisting of a large number of layers. *Appl Math Model* 40:7034–7050
- Chen H, Park E, Hu C (2018) A design solution of PRB with multispecies transport based on a multidomain system. *Environ Earth Sci* 77:630
- Chen JS, Hsu SY, Li MH, Liu CW (2016) Assessing the performance of a permeable reactive barrier-aquifer system using a dual-domain solute transport model. *J Hydrol* 543:849–860
- Chen JS, Ho YC, Liang CP, Wang SW, Liu CW (2019a) Semi-analytical model for coupled multispecies advective-dispersive transport subject to rate-limited sorption. *J Hydrol* 579:124164
- Chen JS, Liang CP, Chang CH, Wan MH (2019b) Simulating three-dimensional plume migration of a radionuclide decay chain through groundwater. *Energies* 12:3740
- van Genuchten MT, Alves WJ (1982) Analytical solutions of the one-dimensional convective-dispersive solute transport equation. U S Department of Agriculture p Technical Bulletin No. 1661
- Goltz M, Huang J (2017) Analytical Modeling of Solute Transport in Groundwater. John Wiley & Sons, Inc.
- Guerrero JSP, Pimentel LCG, Skaggs TH (2013) Analytical solution for the advection-dispersion transport equation in layered media. *Int J Heat Mass Tran* 56:274–282
- Hickson RI, Barry SI, Mercer GN (2009) Critical times in multilayer diffusion. Part 1: Exact solutions. *Int J Heat Mass Tran* 52:5776–5783
- de Hoog FR, Knight JH, Stokes AN (1982) An improved method for numerical inversion of laplace transforms. *SIAM J Sci Stat Comput* 3:357–366
- Kuhlman KL (2013) Review of inverse Laplace transform algorithms for Laplace-space numerical approaches. *Numer Algorithms* 63:339–355
- Leij FJ, van Genuchten MT (1995) Approximate analytical solutions for solute transport in two-layer porous media. *Transp Porous Med* 18:65–85
- Leij FJ, Dane JH, van Genuchten MT (1991) Mathematical analysis of one-dimensional solute transport in a layered soil profile. *Soil Sci Soc Am J* 55:944–953
- Liu C, Ball WP, Ellis JH (1998) An analytical solution to the one-dimensional solute advection-dispersion equation in multi-layer porous media. *Transp Porous Med* 30:25–43
- Mieles J, Zhan H (2012) Analytical solutions of one-dimensional multispecies reactive transport in a permeable reactive barrier-aquifer system. *J Contam Hydrol* 134-135:54–68
- de Monte F (2002) An analytic approach to the unsteady heat conduction process in one-dimensional composite media. *Int J Heat Mass Tran* 45:1333–1343
- Park E, Zhan H (2009) One-dimensional solute transport in a permeable reactive barrier-aquifer system. *Water Resour Res* 45:W07502
- Rodrigo MR, Worthy AL (2016) Solution of multilayer diffusion problems via the Laplace transform. *J Math Anal Appl* 444:475–502
- Sun Y, Wichman IS (2004) On transient heat conduction in a one-dimensional composite slab. *Int J Heat Mass Tran* 47:1555–1559
- Trefethen LN, Weideman JAC, Schmelzer T (2006) Talbot quadratures and rational approximations. *BIT Numer Math* 46:653–670
- Yang B, Liu S (2017) Closed-form analytical solutions of transient heat conduction in hollow composite cylinders with any number of layers. *Int J Heat Mass Tran* 108:907–917
- Zimmerman RA, Jankowski TA, Tartakovsky DM (2016) Analytical models of axisymmetric reaction-diffusion phenomena in composite media. *Int J Heat Mass Tran* 99:425–431